J Mater Sci (2008) 43:3474–3480
DOI 10.1007/s10853-007-2335-x

NANOSMAT 2007 - INTERNATIONAL CONFERENCE ON SURFACES, COATINGS AND NANOSTRUCTURED MATERIALS

Determination of surface properties of various substrates using TiO_2 nanorod coatings with tunable characteristics

Gianvito Caputo · Concetta Nobile · Raffaella Buonsanti · Tobias Kipp · Liberato Manna · Roberto Cingolani · P. Davide Cozzoli · Athanassia Athanassiou

Received: 26 July 2007 / Accepted: 19 November 2007 / Published online: 4 March 2008

Abstract We present a novel approach to cover different substrates with thin light-sensitive layers that consist of organic-capped TiO_2 nanorods (NRs). Such NR-based coatings exhibit an increasing initial hydrophobicity with increasing NR length, and they demonstrate a surface transition from this highly hydrophobic state to a highly hydrophilic one under selective UV–laser irradiation. This behaviour is reversed under long dark storage. Infrared spectroscopy measurements reveal that light-driven wettability changes are accompanied by a progressive hydroxylation of the TiO_2 surface. The surfactant molecules that cover the NRs do not appear to suffer for any significant photocatalytic degradation.

Introduction

In the last years much attention has been focused on the development of new classes of materials that can demonstrate photocatalytic behaviour and reversible wettability properties under proper light illumination, for applications in diverse technological fields. For these purposes titanium dioxide (TiO_2) represents one of the most studied and widely used material due to its low cost, enhanced stability, and easy way of preparation [1–7].

The photocatalytic activity of TiO_2 has attracted much attention, and different mechanistic and chemical pathways have been proposed to explain it, since it has found numerous applications, such as, in the degradation of organic pollutants, in solar energy conversion, and in the damage of malignant cells by photodynamic therapy [8, 9].

The photocatalytic activity of the TiO_2 thin films is often coupled with another intriguing property, its switchable wettability [10–17]. A general mechanistic explanation of this interesting phenomenon is based on the photogeneration of excited charge carriers (i.e., electrons and holes) with a strong red-ox activity when TiO_2 absorbs light of energy equal to, or greater than, its band gap energy. As a consequence of photoexcitation, oxygen vacancies are created on the surface, while Ti^{4+} sites are reduced to Ti^{3+}. The induced defects are able to coordinate to water, either by chemisorption that leads to water decomposition into OH groups, or by undissociative physisorption. Both processes can further promote adhesion of water multilayers through formation of hydrogen bonds. In both cases, a highly hydroxylated surface is produced [12–14]. This mechanism leads to a surface transition from a quite hydrophobic state to a very hydrophilic one upon UV irradiation [18, 19]. The water contact angle is slowly recovered upon subsequent dark storage, and it can be accelerated upon thermal or ultrasound treatments [11–13]. The possibility to tune the wettability changes is appealing for applications, such as, the fabrication of self-cleaning, antifogging, and antireflective surfaces [20].

G. Caputo (✉) · C. Nobile · R. Buonsanti · L. Manna · R. Cingolani · P. D. Cozzoli · A. Athanassiou
NNL—National Nanotechnology Laboratory of INFM-CNR, Via Arnesano, 73100 Lecce, Italy
e-mail: gianvito.caputo@unile.it

A. Athanassiou
e-mail: Athanassia.Athanassiou@unile.it

G. Caputo · C. Nobile · R. Buonsanti · P. D. Cozzoli
Scuola Superiore ISUFI, Distretto Tecnologico, University of Salento, Via Arnesano, 73100 Lecce, Italy

T. Kipp
Institut fur Angewandte Physik und Zentrum fur Mikrostrukturforschung, Universitat Hamburg, Jungiusstrasse 11, 20355 Hamburg, Germany

Several efforts have been devoted to the preparation of TiO_2 thin films for switchable wettability. The most commonly used technique is the metallorganic chemical vapour deposition (MOCVD), usually performed in a magnetron-sputtering device. Some reports referred to this technique deal with the doping of TiO_2 with rare earth elements or nitrogen, which extend the oxide absorption to the visible region, allowing the use of irradiation of lower energy [21–25]. The high temperature processing, ranging from 400 to 500 °C, ensures coatings with negligible carbon contents and a high degree of crystallinity. However, this type of treatment cannot be applied to thermolabile substrates, such as polymers. Moreover, losses in photocatalytic efficiency and in turn, in photowettability, are frequently encountered due to undesired crystal phase transitions [24, 25].

Colloidal suspensions of titanium alkoxide compounds in combination with layer-by-layer assembly have been employed for the preparation of polycrystalline films, which are achieved after heating the substrates in air or under nitrogen at high temperature, that is a fundamental requirement for the removal of all the organic moieties. In these cases, the photoinduced differences in contact angle can be very low if the starting material presents a flat surface [26–31].

In this work, we report the preparation of photoresponsive coatings with reversible wetting properties using organic-capped anatase TiO_2 nanorods (NRs). Due to their anisotropic shape, the NRs have a higher surface-to-volume ratio, compared to nanospheres with identical volume. Therefore, NRs possess more surface active sites available for surface reactions, and can facilitate an increased delocalization of charge carriers along their length [32, 33]. We present the deposition of uniform and optically transparent thin films from an aqueous suspension of TiO_2 NRs of different sizes on a variety of substrates, such as, ITO, silicon and polymers (PS and PMMA). We demonstrate that the initial hydrophobicity of the samples increases with increasing NR aspect ratio, and that the prepared coatings exhibit a fully reversible hydrophobic–hydrophilic behaviour upon laser pulsed ultraviolet irradiation and dark storage cycles.

Experimental section

Materials

All chemicals were of the highest purity available and used as received. Titanium tetrachloride ($TiCl_4$, 99.999%), oleic acid ($C_{17}H_{33}CO_2H$ or OLAC, 90%), 1-octadecene ($C_{18}H_{36}$ or ODE, 90%), oleyl amine ($C_{17}H_{33}NH_2$ or OLAM, 70%), polymethylmethacrylate (PMMA, $M_W = 120.000$), and polystyrene (PS, $M_W = 88.000$) were purchased from Aldrich. Water was bidistilled (Millipore Q). Silicon (100) p-type slabs were purchased from *Jocam*. Indium tin oxide (ITO) substrates were purchased from *Praezisions Glas & Optik GmbH*.

Synthesis

Organic-capped TiO_2 NRs were prepared by a modified nonaqueous approach as follows [34]: ODE (10 mL), OLAC (2 mmol) and OLAM (10 mmol) were loaded in a three-necked-flask. The solution was degassed at 120 °C for 1 h under vigorous stirring and then switched under nitrogen flow. The temperature was raised up to 280 °C and 1 mmol of $TiCl_4$ was rapidly injected into the mixture. The reaction was allowed to proceed for 30 min. After being cooled down, the NRs were precipitated upon addition of acetone and 2-propanol, separated by centrifugation, and washed twice in order to remove the surfactant excess. After this procedure the NRs were redissolved in toluene, providing an optically transparent solution.

Preparation of TiO_2 coatings

Typically the TiO_2 NR thin films were deposited onto silicon, ITO, and polymeric substrates (e.g., PS and PMMA) by dipping them into an aqueous suspension of TiO_2 NRs. The prepared coatings then were dried and stored at room temperature.

Irradiation experiments

In order to change the wettability of the TiO_2 thin films, they were irradiated with the third harmonic wavelength (355 nm) of a Nd-YAG laser, with pulse duration of 3 ns, repetition rate of 10 Hz, at energy density of 6 mJ cm^{-2}, for 120 min (72,000 pulses).

Characterization

Low-resolution Transmission Electron Microscopy (TEM) images of the freshly synthesized TiO_2 NRs were collected with a Jeol Jem 1011 microscope using an accelerating voltage of 100 kV. For these measurements, a few drops of a dilute NR solution were deposited on carbon-coated copper grids and observed after the solvent evaporation.

X-ray diffraction (XRD) patterns of TiO_2 NR powders were collected with a Philips X'Pert diffractometer in Bragg-Brentano reflection geometry using filtered Cu $K\alpha$ radiation ($\lambda = 1.54056$ Å). For XRD measurements, the dried TiO_2, NR powders were placed on an silicon sample holder.

Scanning electron microscopy (SEM) characterization of TiO_2 coatings deposited onto silicon substrates was

performed with a RAITH 150 EBL instrument. Typically, the images were acquired at low accelerating voltages (<5 kV).

Raman spectroscopy experiments were performed at room temperature on the TiO_2-coated substrates by using a diode-pumped solid state laser (at $\lambda = 532$ nm) that was coupled into an optical microscope with a 10× objective lens, which focused a 8-μm sized light spot onto the sample surface. The Raman scattered light was collected by the same objective and spectrally analyzed by a triple Raman spectrometer (Dilor XY, with a resolution of about 1 cm^{-1}) equipped with a Peltier-cooled deep-depletion CCD detector. Typical acquisition times were of the order of 30–60 s.

Fourier Transform Infrared Spectroscopy (FT-IR) measurements in the 4,000–400 cm^{-1} spectral range were carried out on TiO_2-coated ITO substrates using a Bruker Equinox 70 FT-IR apparatus in transmission mode at a resolution of 4 cm^{-1}.

Water contact angle (WCA) characterization was performed on the TiO_2 coatings by the sessile drop method using a CAM200-KSV instrument.

Results and discussion

Figure 1 shows TEM images of the TiO_2 NRs, whose average length can be modulated from 50 to 200 nm (panels a, b, c). The shorter NRs are characterized by a rod-like profile, and the longer ones exhibit arrow-shaped terminations.

According to Raman measurements performed on the NRs thin films on silicon, presented in panel a of Fig. 2, the NRs occur in the anatase (tetragonal) phase structure. In agreement with the literature, the strongest peak associated to E_g vibrational mode is centred at 151 cm^{-1} and the other two less intense peaks are located at 200 and 644 cm^{-1}. One B_{1g} peak is observed at 401 cm^{-1}, and another formed by the overlapping of the B_{1g} and A_{1g} vibrational modes is shown at 517 cm^{-1} [35–37]. These results are further supported by routine XRD analyses, an example of which is reported in panel b of Fig. 2. The XRD profile is consistent with the standard pattern of the tetragonal anatase TiO_2 polymorph. The comparatively higher intensity and narrower width of the (004) reflection indicate a preferential crystal elongation along the *c*-axis direction, as found previously [34].

In Fig. 3, SEM images of different NR films deposited on silicon substrates are shown at the same magnification. It can be observed that especially the shorter NRs present a certain degree of lateral alignment on the surface where they are arranged closely packed. Moreover, the formed films appear to be rather uniform, without significant density of cracks. Although the degree of packaging of

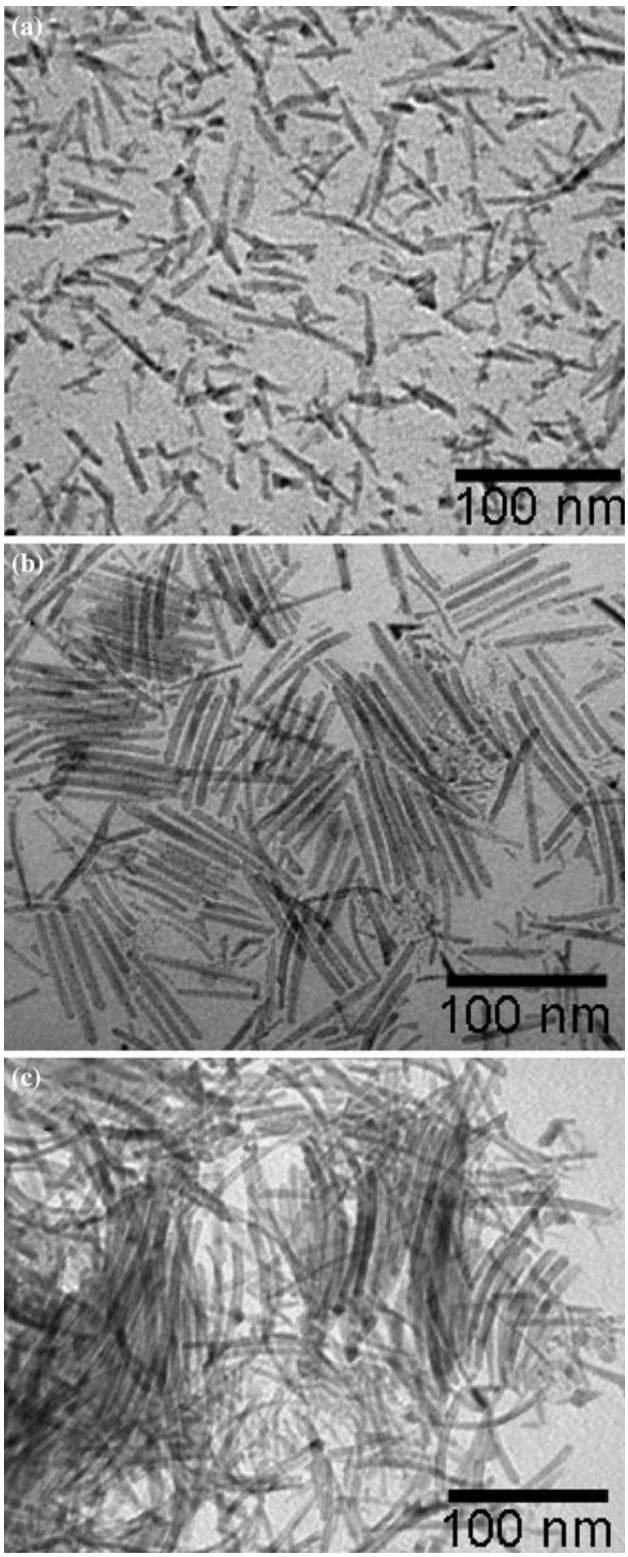

Fig. 1 Low-resolution TEM images of TiO_2 NRs with different mean length (**a**) 50 nm, (**b**) 100 nm, and (**c**) 200 nm

NRs is similar for all the samples, the films prepared by the longer and less regularly shaped NRs exhibit increased surface roughness, since such NRs can have various

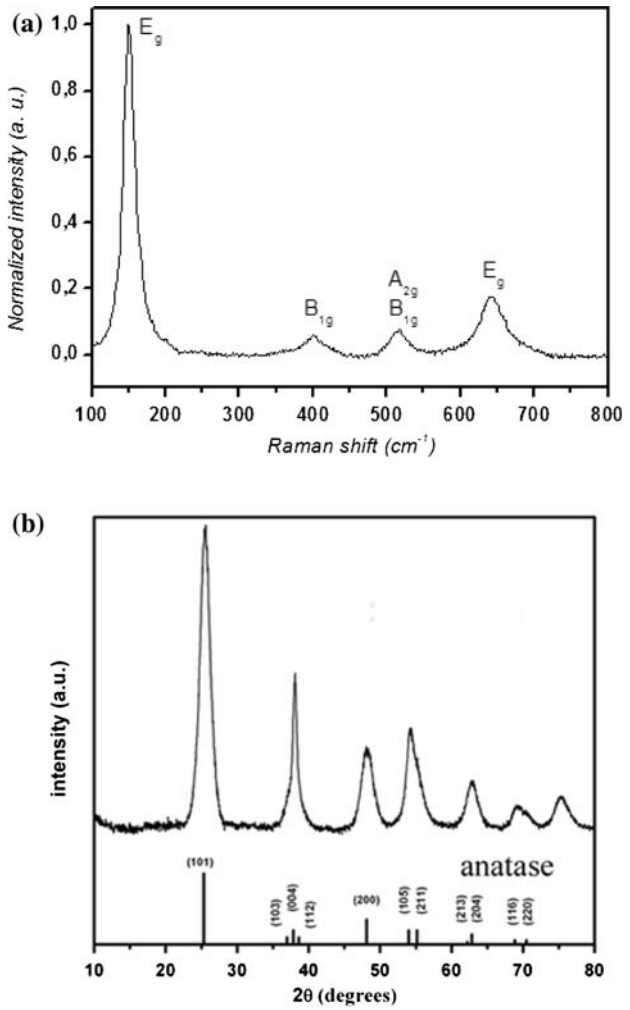

Fig. 2 (**a**) Typical Raman spectrum of the films formed by the organic-capped TiO_2 NRs and (**b**) typical XRD pattern of TiO_2 NR powders

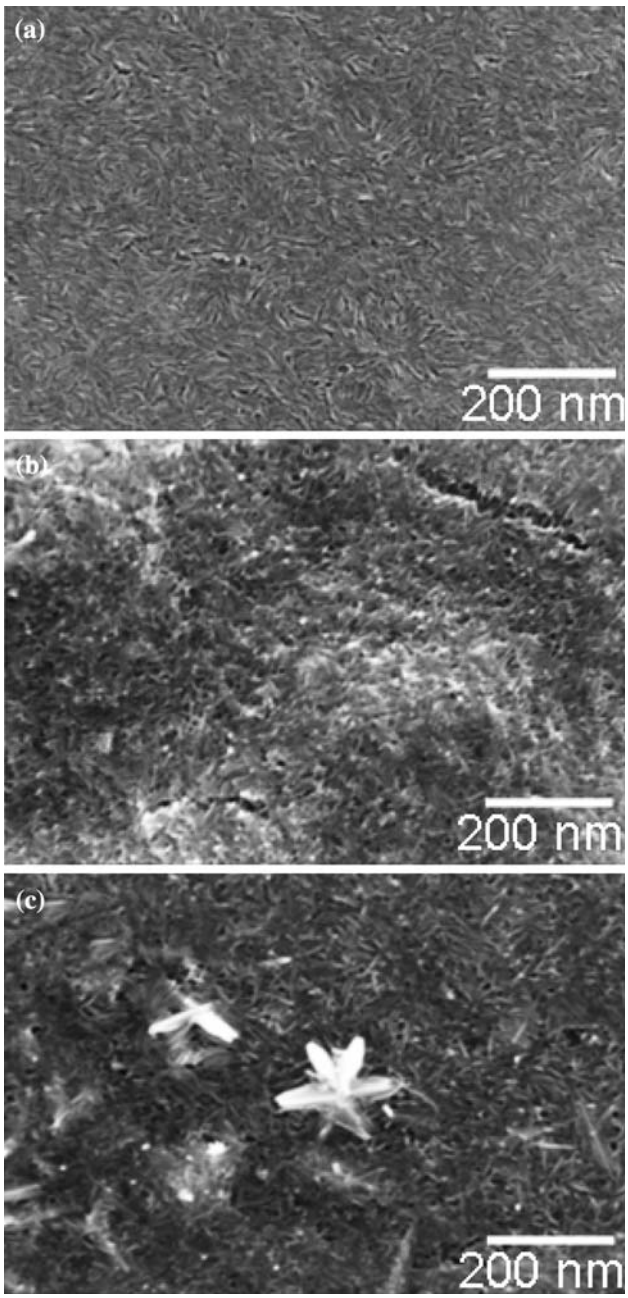

Fig. 3 SEM images of TiO_2 films deposited onto a silicon substrate from NRs with different mean lengths: (**a**) 50 nm, (**b**) 100 nm, and (**c**) 200 nm

orientations with respect to the substrate, occasionally forming aggregates with flower-like morphology (panel c).

Figure 4 reports the WCA measurements performed on the TiO_2 NR coatings deposited on silicon substrates, before irradiation, immediately after the UV irradiation, and after prolonged dark storage. The initial contact angle of the NR films is remarkably increased compared the one measured on flat and bare TiO_2 anatase films (40–50°). This is due to the fact that the NRs are partially covered by hydrophobic organic capping molecules (i.e., the surfactants used in their synthesis), and that the NR-based films exhibit significant nanometer-scale roughness. Furthermore, it can be observed that the starting hydrophobicity of the coatings prepared from the longer NRs is improved by more than 10° compared to the one of the short NRs. This is due to the aforementioned higher roughness that characterizes these surfaces, as demonstrated by the SEM investigation of Fig. 3c. The relationship connecting the WCA of the films with their surface roughness is described by the Cassie–Baxter model, developed to describe the wettability of rough surfaces. According to this model, only partial wetting of rough surfaces may occur due to the trapping of air underneath the drop at the recessed regions of the surfaces. The contact angle, θ_r, of a liquid droplet is an average between the value that would be measured on air (i.e., 180°) and the value, θ, that would be measured on the corresponding flat surface. Since the drop is situated

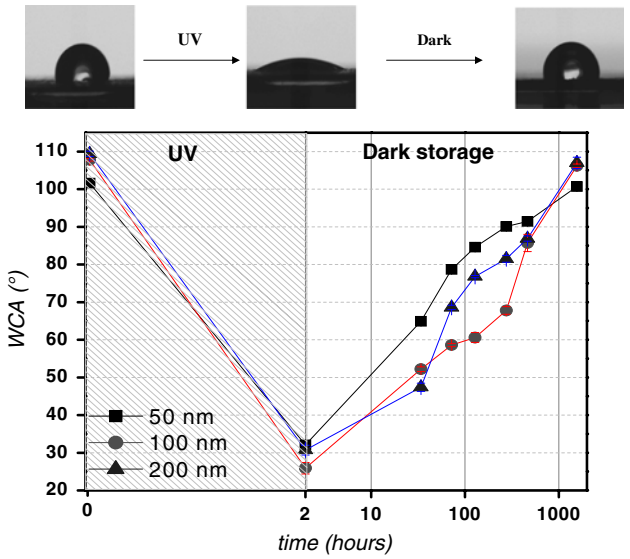

Fig. 4 Reversible changes in WCA measured for TiO_2 films made of NRs of different mean lengths (50, 100, and 200 nm) upon a cycle of UV irradiation and dark storage. The *x*-axis appears in logarithmic scale

partially on air, the rough surface always exhibits a higher contact angle compared to the corresponding flat surface, which increases with increasing roughness. The model is described by:

$$\cos\theta_r = f(1 + \cos\theta) - 1, \quad (1)$$

where $f \leq 1$ is the solid fraction of the surface in contact with the liquid which decreases with increasing surface roughness, θ is the contact angle of a liquid on a flat surface, and θ_r is the contact angle of a liquid on a rough surface of the same chemistry [38].

As shown in Fig. 4, after irradiation of the thin films with UV laser pulses at 355 nm for 120 min, the initially hydrophobic surfaces become very hydrophilic, reaching a WCA as low as 35°–25°, depending on the type of NRs used.

FT-IR spectroscopy was used to investigate the chemical behaviour of the films exposed to UV irradiation in order to understand the mechanism of the decrease in the WCA. In panel a of Fig. 5, the FT-IR spectra of the as-prepared NRs exhibit the intense C–H stretching vibrations of the $–CH_2–$ and $–CH_3$ moieties of OLAC-OLAM alkyl chain in the 2960–2860 cm^{-1} range. A very weak but distinct peak for the olefinic =C–H stretching is visible at 3008 cm^{-1}. Additionally, it can be noted that the C–H vibrations are superimposed on the low-energy side of a broad and weak O–H stretching band centred at 3500 cm^{-1}, which comprises the contributions from terminal titanol groups (i.e., TiO–H moieties) and molecularly physisorbed H_2O. Consistently with the latter assignments, a weak shoulder for the H_2O bending can be observed at around 1640–1620 cm^{-1}. In addition, the characteristic antisymmetric and

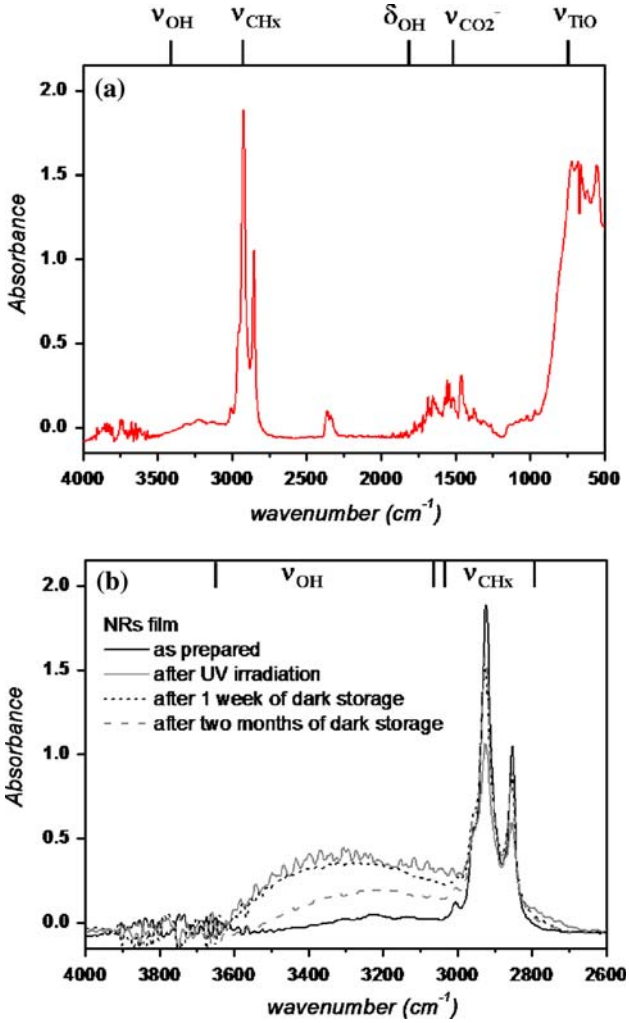

Fig. 5 FT-IR spectra of the TiO_2 NR coatings: (**a**) as prepared and (**b**) after UV irradiation and subsequent dark storage for different time periods

symmetric stretching vibrations of carboxylate anions at 1520 and 1435 cm^{-1}, respectively, indicate that the OLAC ligands are bound to TiO_2 surface in a chelating bidentate mode. Finally, the intense and broad raise in absorption below 1000 cm^{-1} is due to the Ti–O–Ti stretching of the anatase lattice. All of these assignments are in agreement with previous FT-IR studies on carboxylate-capped TiO_2 nanorods prepared by other approaches [39]. As shown in panel b of Fig. 5, following UV irradiation a considerable growth of the hydroxyl stretching signal centred at 3500 cm^{-1} is detectable, that is attributable to an increase in the surface density of Ti–OH moieties [11–14]. The higher hydroxylation degree of the surface allows for the spreading of the water droplets, explaining the remarkably lower WCA values measured after irradiation. After dark storage for 2 months, the occurrence of dehydroxylation process on the TiO_2 surface is evidenced by the clear decrease in the Ti–OH stretching band. As a macroscopic

evidence of these chemical modifications, the WCA almost recovers its initial value as shown in Fig. 4.

Moreover, it can be observed that the alkyl chain of the OLAC–OLAM surfactants stretching signals undergo a significant decrease upon UV irradiation. These signals recover their intensity after the dark storage. This recovery cannot be due to the adsorption of any organic compounds present in the environment, as confirmed by our control experiments. We tentatively propose that these reversible changes in the infrared absorption can be ascribed to the surfactant molecules undergoing conformational rearrangements in response to the TiO_2 surface hydroxylation/dehydroxylation process. Therefore, we assume that negligible photocatalytic degradation of the surfactant molecules which surround the NRs occurs under our irradiation experiments. Most of the studies on the photocatalysis of TiO_2 are accomplished by using continuous wave UV lamps, so that the generation of the oxidant radicals which are responsible for the degradation of organic compounds is continuous over time. On the contrary, recent experiments on the decay times of photogenerated carriers in TiO_2 nanoparticle films demonstrate that photocatalysis can be inhibited under a pulsed irradiation regime, similar to that employed in this work, due to electron-hole recombination occurring during the time interval between consecutive laser pulses [40].

These experiments are in perfect agreement with the mechanistic pathways that have been proposed in the literature to explain the hydrophobic to hydrophilic conversion of a TiO_2 surface. When UV light irradiates a TiO_2 surface, a photogenerated hole reacts with lattice oxygen and forms an oxygen vacancy, to which water can coordinate both molecularly and dissociatively. In the latter case, the hydroxylated surface is attained in an energetically metastable state, since after dark storage, the atmospheric oxygen replaces the hydroxyl groups on the TiO_2 surface, finally leading to the recovery of the initial hydrophobic state [41–43].

Finally, it is worth mentioning here that the observed reversible wettability changes are similar to those obtained on TiO_2 NR coatings deposited on both ITO and polymeric substrates. Since TiO_2 strongly absorbs the UV wavelengths, it further contributes to protect such polymer substrates from any UV driven modification, such as bond cleavage or photodegradation.

Conclusions

To summarize, we succeeded to coat different substrates with TiO_2 films using TiO_2 NRs with different dimensions. As the length of the NRs was increased, we observed an increase in the roughness of the coatings. The latter made the films very hydrophobic, thus affecting their wetting behaviour. We checked the reversible wettability of the films upon UV–laser irradiation and dark storage cycles. The WCA decreased down to 25–35° after UV irradiation and it recovered its initial value after dark storage for more than 2 months. FT-IR measurements showed that the mechanism responsible for this behaviour is strictly connected to the hydroxylation degree achieved on the UV-irradiated surfaces.

References

1. Zhang Z, Wang CC, Zakaria R, Ying JY (1998) J Phys Chem B 102:10871
2. Kominami H, Muratami S, Kato J, Kera Y, Ohtani B (2002) J Phys Chem B 106:10501
3. O' Regan B, Gratzel M (1991) Nature 353:737
4. Nakade S, Matsuda M, Kambe S, Saito Y, Kitamura T, Sakata T, Wada Y, Mori H, Yanagida S (2002) J Phys Chem B 106:10004
5. Nelson J, Haque SA, Klug DR (2001) Phys Rev B 63:205
6. Nelson J (1999) Phys Rev B 59:23
7. Zhu Y, Shi J, Zhang Z, Zhang C, Zhang X (2002) Anal Chem 74:120
8. Fujishima A, Honda K (1972) Nature 238:37
9. (a) Moser WR (1990) Advanced catalysis and nanostructured materials. Academic Press, San Diego; (b) Schiavello M (1988) Photocatalysis and environment, trends and applications. Kluwer, Dordrecht; (c) Pelizzetti E, Serpone N (1989) Photocatalysis. Fundamentals and applications. Wiley, New York
10. Liang LF, Feng X, Liu J, Rieke PC, Fryxell GE (1998) Macromolecules 31:7845
11. Sakai N, Wang R, Fujishima A, Watanabe T, Hashimoto K (1998) Langmuir 14:5918
12. Wang R, Sakai N, Fujishima A, Watanabe T, Hashimoto K (1999) J Phys Chem B 103:2188
13. Nakajima A, Watanabe T, Hashimoto K (2001) J Photochem Photobiol A Chem 146:129
14. Sakai N, Fujishima A, Watanabe T, Hashimoto K (2001) J Phys Chem B 105:3023
15. Nakajima A, Koizumi S, Watanabe T, Hashimoto K (2000) Langmuir 16:7048
16. Sakai N, Fujishima A, Watanabe T, Hashimoto K (2003) J Phys Chem B 107:1028
17. Miyauchi M, Nakajima A, Fujishima A, Hashimoto K, Watanabe T (2000) Chem Mater 12:3
18. Wang R, Fujishima A, Chikuni M, Kojima E, Kitamura A, Shimohigoshi M, Watanabe T (1997) Nature 388:431
19. Wang R, Fujishima A, Chikuni M, Kojima E, Kitamura A, Shimohigoshi M, Watanabe T (1998) Adv Mater 10:135
20. Parkin IP, Palgrave RG (2005) J Mater Chem 15:1689
21. Rampaul A, Parkin IP, O'Neill SA, DeSouza J, Mills A, Elliott N (2003) Polyhedron 22:35
22. Sirghi L, Hatanaka Y (2003) Surf Sci 53:L323
23. Luca D, Mardare D, Iacomi F, Teodorescu CM (2006) Appl Surf Sci 252:6122
24. Kemmitt T, Al-Salim NI, Waterland M, Kennedy VJ, Markwitz A (2004) Curr Appl Phys 4:189
25. Mills A, Elliott N, Parkin IP, O'Neill SA, Clark RJ (2002) J Photochem Photobiol A Chem 151:171
26. Yu J, Zhao X, Zhao Q, Wang G (2001) Mater Chem Phys 68:253
27. Yu JC, Yu J, Ho W, Zhao J (2002) J Photochem Photobiol A Chem 148:331

28. Dag O, Soten I, Celik O, Polarz S, Coombs N, Ozin GA (2003) Adv Funct Mater 13:30
29. Gao Y, Masuda Y, Koumoto K (2004) Langmuir 20:3188
30. Cebeci FC, Wu Z, Zhai L, Cohen RE, Rubner MF (2006) Langmuir 22:2856
31. Allain E, Besson S, Durand C, Moreau M, Gacoin T, Boilot JP (2007) Adv Funct Mater 17:1
32. Manna L, Scher EC, Li LS, Alivisatos AP (2002) J Am Chem Soc 124:7136
33. Nelson J (2002) Curr Opin Solid State Mater Sci 6:87
34. Seo JW, Jun YW, Ko SJ, Cheon J (2005) J Phys Chem B 109:5389
35. Xu WX, Zhu S, Fu XC, Chen X (1999) Appl Surf Sci 148:253
36. Bersani D, Lottici PP, Ding XZ (1998) Appl Phys Lett 72:73
37. Xu CY, Zhang PX, Yan L (2001) J Raman Spectrosc 32:862
38. Cassie ABD, Baxter S (1944) Trans Faraday Soc 40:546
39. Cozzoli PD, Kornowski A, Weller H (2003) J Am Chem Soc 125:14533
40. Murai M, Tamaki Y, Furube A, Hara K, Katoh R (2007) Catal Today 120:214
41. Finnie KS, Cassidy DJ, Bartlett JR, Woolfrey JL (2001) Langmuir 17:816
42. Panayotov DA, Yates JT (2005) Chem Phys Lett 410:11
43. Wang C, Groenzin H, Shultz MJ (2003) Langmuir 19:7330